A study on the energy transfer of a square prism under fluid-elastic galloping

H.G.K.G. Jayatunga, B.T. Tan, J. S. Leontini

Abstract

Extracting useful energy from flow induced vibrations has become a developing area of research in recent years. In this paper, we analyse power transfer of an elastically mounted body under the influence of aeroelastic galloping. The system and the power transfer is analysed by numerically integrating the quasi-steady state model equations. The power transfer is analysed for both high ($Re = 22300$) and low ($Re = 165$) Reynolds numbers cases, and the impact of the system mass is investigated for both.

At high mass ratios ($m^* > 50$), the power transfer is completely controlled by galloping and essentially independent of the mass. A combined mass-damping coefficient, Π_2, that can be derived from the equation of motion, is shown to be the parameter that governs power output. The system is a balance between the power delivered to the system due to hydrodynamic forcing and power removed through mechanical damping which are governed by the hydrodynamic forcing characteristics (i.e. the lift force as a function of incident angle) and mechanical damping coefficient respectively. The peak efficiency of 0.26% for $Re = 165$ and 6.7% for $Re = 22300$ were observed when the non-dimensionalised mass-damping factor becomes 0.314 and 1.04 respectively.

A contradictory behaviour is observed at low m^* between the low and high Re cases. The forcing due to vortex shedding at low Reynolds numbers suppresses the galloping excitation and results in a reduced power output. For the case with high Re power output increases as m^* is reduced . For this high Re case, at low m^* the reduction in inertia allows the body to accelerate faster and spend a larger portion of the period at relatively high transverse velocities. Extrapolating this trend, the limit to peak efficiency is found to be 13.5% and occurs when $m^* \to 0$ and $U^* \to \infty$ and $\Pi_2 = 1.22$

Keywords:

1. Introduction

Fluid-elastic galloping is one of the sub-areas of research in fluid structure interactions. This area has been of interest due to the vibrations crated by galloping on transmission lines and civil structures and leading them to failure. Therefore understanding this phenomenon in order to suppresses these vibrations was quite important. However, the search for alternate energy sources with minimal environmental impact has become an important area of research in the modern word. Therefore researchers are moving towards investigating

the possibility of extracting useful energy from this vibrations rather than suppressing them. Thus, it is quite important to understand the governing parameters and analyse the influence of them on the energy transfer from the fluid to the structure, because this understanding will lead to develop better practical applications. Hence, in this paper we focus on understanding the energy transfer from the fluid to the body and isolate the governing parameters influencing it.

According to **?**, **?** provided a criterion for galloping by considering the auto-rotation of an aerofoil. **?** provided a theoretical explanation for galloping for iced electric transmission lines. A weakly non-linear theoretical aeroelastic model to predict the response of galloping was developed by **?** based on the quasi-steady state hypothesis. Experimental lift and drag data on a fixed square prism at different angles of attack were used as an input for the theoretical model. It essentially used a curve fit of the transverse force to predict the galloping response. The study managed to achieve a good agreement with experimental data.

However, the QSS model equation when solved analytically using the sinusoidal solution, cannot predict the response for cases with low mass ratios. **?** observed that finite element simulations show a sudden change in amplitude below a critical value of the mass ratio. The quasi-oscillator equation in **?** was altered to account for the vortex shedding and solved numerically to predict the reduced displacement amplitude at low mass ratios to the point where galloping is no longer present. **?** investigated the possibility of extracting power from vibrations caused by galloping using the quasi-steady state model. So far the studies on galloping using quasi-steady state assumption has been mainly focused on understanding the behaviour of the displacement amplitude. Although, it is quite important to analyse the behaviour of the velocity when studying the power transfer from the fluid to the body. This is because power could be simply defined as the product the force and velocity. This study also focuses on how well the QSS model perform at high damping at low Reynolds numbers.

Here, the modified QSS model developed by **?** is integrated numerically for low Reynolds numbers. The power transfer from the fluid to the structure and the influence of mechanical parameters was investigated (i.e. mass, stiffness and damping). To this end, a series of previously mentioned mechanical parameters are tested at two different values of Re: $Re = 200$, a case that should remain laminar and closer to two-dimensional behaviour; $Re = 22300$, a case where the flow is expected to be turbulent and three-dimensional. Both cases require the input of transverse force coefficients C_y as a function of angle of attack θ for a fixed body. These data are provided from direct numerical simulations for the $Re = 200$ case, while the data provided by **?** are used for the $Re = 22300$ case.

Nomenclature

|	
a_1, a_3, a_5, a_7	coefficients of the polynomial to determine C_y
A	displacement amplitude
c	damping constant
D	characteristic length (side length) of the cross section of the body
$f = \sqrt{k/m}/2\pi$	natural frequency of the system
F_y	instantaneous force normal to the flow
F_0	amplitude of the oscillatory force due to vortex shedding
k	spring constant
m	mass of the body
m_a	added mass
P_d	power dissipated due to mechanical damping
$P_{in} = \rho U^3 D/2$	Energy flux of the approaching flow
P_{mean}	mean power
P_t	power transferred to the body by the fluid
t	time
U	freestream velocity
U_i	Induced velocity
$y, \dot{y}, \ddot{y}$	transverse displacement, velocity and acceleration of the body
$\mathcal{A} = DL$	frontal area of the body
λ	Inverse time scale of a galloping dominated flow
$\lambda_{1,2}$	Eigenvalues of linearized equation of motion
ρ	fluid density
$\omega_n = 2\pi f$	natural angular frequency of the system
ω_s	vortex shedding angular frequency
$c^* = cD/mU$	non-dimensionalised damping factor
$C_y = F_y/0.5\rho U^2 DL$	normal (lift) force coefficient
$m^* = m/\rho D^2 L$	mass ratio
Re	Reynolds number
$U^* = U/fD$	reduced velocity
$Y = y/D$	non-dimensional transverse displacement
$\dot{Y} = m^* \dot{y}/a_1 U$	non-dimensional transverse velocity
$\ddot{Y} = m^{*2} D/a_1^2 U^2$	non-dimensional transverse acceleration
$\Gamma_1 = 4\pi^2 m^{*2}/U^{*2} a_1^2$	First dimensionless group arising from linearised, non-dimensionalised equa
$\Gamma_2 = c^* m^*/a_1$	Second dimensionless group arising from linearised, non-dimensionalised equ
$\zeta = c/2m\omega_n$	damping ratio
$\theta = \tan^{-1}(\dot{y}/U)$	instantaneous angle of incidence (angle of attack)
$\Pi_1 = 4\pi^2 m^{*2}/U^{*2}$	Combined mass-stiffness parameter
$\Pi_2 = c^* m^*$	Combined mass-damping parameter
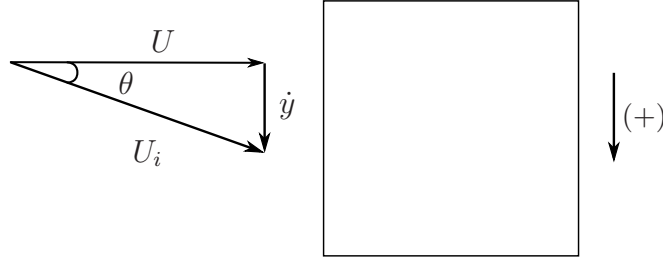
Figure 1: Induced angle of attack on the square prism due to the resultant of free-stream velocity of the fluid and transverse velocity of the body.

2. Problem formulation and methodology

2.1. The quasi-steady state (QSS) model

The equation of motion of the body is given by

$$(m)\ddot{y} + c\dot{y} + ky = F_y, \tag{1}$$

where the forcing term F_y is given by

$$F_y = \frac{1}{2}\rho U^2 \mathcal{A} C_y. \tag{2}$$

In the QSS model, it is assumed that the force on the body at a given instantaneous incident angle θ (defined in figure 1) is the same as the mean force on a static body at the same incident angle, or angle of attack. The instantaneous value of C_y is therefore determined by an interpolating polynomial based on the lift data for flow over a stationary body at various θ. Using the relationship between θ and the instantaneous transverse velocity of the body $\dot{y}$ shown in figure 1, C_y can be written as a function of $\dot{y}$. The order of the interpolation polynomial used to define this function has varied from study to study. For example a 7th order polynomial was used in **?** and 3rd order polynomial was used in **?**. **?** concluded that using a 7th order polynomial is sufficient and a polynomial higher than that of 7th order doesn't provides a significantly better result. Thus a 7th order interpolating polynomial is used in this present study. As a result, $C_y(\theta)$ (noting that theta is proportional to $\dot{y}/U$) is defined as

$$C_y(\theta) = a_1 \left(\frac{\dot{y}}{U}\right) + a_3 \left(\frac{\dot{y}}{U}\right)^3 + a_5 \left(\frac{\dot{y}}{U}\right)^5 + a_7 \left(\frac{\dot{y}}{U}\right)^7. \tag{3}$$

It is expected that vortex shedding will be well correlated along the span and provide significant forcing at low Re. **?** introduced an additional sinusoidal forcing function to the hydrodynamic forcing to model this. This enables the model to provide accurate predictions even at low mass ratios where galloping excitation is suppressed or not present. In this study, the forcing due to vortex shedding in low Re cases is incorporated using a

4

sinusoidal forcing function $F_0 \sin \omega_s t$ added to the right-hand side of equation 1. Here, ω_s and F_0 represent the angular vortex shedding frequency and the maximum force due to shedding respectively. Thus, the final equation for the modified QSS model is

$$m\ddot{y}+c\dot{y}+ky=\frac{1}{2}\rho U^2 \mathcal{A}\left(a_1\left(\frac{\dot{y}}{U}\right)+a_3\left(\frac{\dot{y}}{U}\right)^3+a_5\left(\frac{\dot{y}}{U}\right)^5+a_7\left(\frac{\dot{y}}{U}\right)^7\right)+F_0\sin\left(\omega_s t\right). \quad (4)$$

This equation can be solved using standard time integration methods. In this study the fourth-order Runge-Kutta scheme built in to the MATLAB routine 'ode45' was generally used to obtain the solutions.

2.2. Calculation of average power

The dissipated power due to the mechanical damping represents the ideal potential amount of harvested power output. Therefore, the mean power output can be given by

$$P_{mean} = \frac{1}{T}\int_0^T (c\dot{y})\dot{y}dt, \quad (5)$$

where T is the period of integration and c is the mechanical damping constant.

It should be noted that this quantity is equal to the work done on the body by the fluid, defined as

$$P_{mean} = \frac{1}{T}\int_0^T F_y\dot{y}dt, \quad (6)$$

where F_y is the transverse (lift) force.

These two definitions show two important interpretations of the power with respect to any energy production device. The first shows that power will be high for situations where the damping coefficient is high, and the transverse velocity is consistently high. The second shows that power will be high for situations where the transverse force and the body velocity are in phase.

Case	a_1	a_3	a_5	a_7
Re=165	1.97	71.28	-6937	-25943
Re=22300	2.69	168	1670	59900

Table 1: Coefficient values used in the 7th order interpolation polynomial for high ($Re = 22300$) and low ($Re = 165$) Reynolds numbers. These data are used as input data to calculate the right-hand side of Eq. 4 throughout this study.
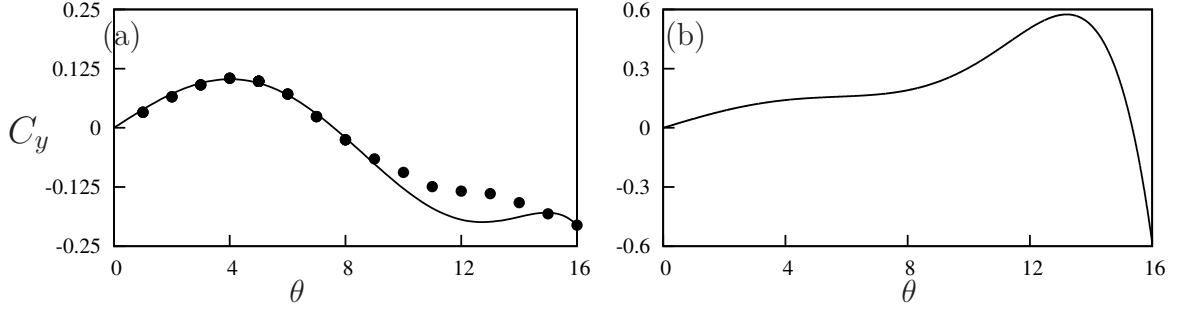
Figure 2: Lift coefficient, C_y, as a function of incidence angle θ, for a static square cross section. (a) Data from simulations at $Re = 165$ (b) data from ? at $Re = 22300$. Points (•) are measurements from the simulations. The solid lines in both plots are 7th-order interpolating polynomial used to predict the fluid forcing for the QSS model. C_y is the force coefficient of the force which occurs normal to the induced velocity.

2.3. Validation

3. Results

The natural time scales of the system can be found by solving for the eigenvalues of the linearised equation of motion, namely

$$(m)\ddot{y}+c\dot{y}+ky=\frac{1}{2}\rho U^2 \mathcal{A}a_1\left(\frac{\dot{y}}{U}\right), \tag{7}$$

which is simply the equation of motion presented in equation 4 with the polynomial series for the lift force truncated at the linear term, and the forcing term representing vortex shedding removed.

Combining the $\dot{y}$ terms and solving for eigenvalues gives

$$\lambda_{1,2} = -\frac{1}{2}\frac{c-\frac{1}{2}\rho U \mathcal{A}a_1}{(m)} \pm \frac{1}{2}\sqrt{\left[\frac{c-\frac{1}{2}\rho U \mathcal{A}a_1}{(m)}\right]^2 - 4\frac{k}{(m+m_a)}}. \tag{8}$$

If it is assumed that the spring is relatively weak, $k \to 0$, a single non-zero eigenvalue remains. This eigenvalue is

$$\lambda = -\frac{c-\frac{1}{2}\rho U \mathcal{A}a_1}{(m)}. \tag{9}$$

Further, if it is assumed that the mechanical damping is significantly weaker than the aerodynamic forces on the body, $c \to 0$ and

$$\lambda = \frac{\frac{1}{2}\rho U \mathcal{A}a_1}{(m)}. \tag{10}$$

In this form, λ represents the inverse time scale of the motion of the body due to the negative damping effect of the long-time aerodynamic forces. In fact, the terms can be regrouped and λ written as

$$\lambda = \frac{a_1}{m^*}\frac{U}{D} \tag{11}$$

6

Written this way, the important parameters that dictate this inverse time scale are clear. The rate of change in the aerodynamic force with respect to angle of attack when the body is at the equilibrium position, $\partial C_y/\partial \alpha$, is represented by a_1. The mass ratio is represented by m^*. The inverse advective time scale of the incoming flow is represented by the ratio U/D. Increasing a_1 would mean the force on the body would increase more rapidly with small changes in the angle of attack, θ, or transverse velocity. Equation 11 shows that such a change will increase the inverse time scale, or analogously decrease the response time of the body. Increasing the mass of the body, thereby increasing m^*, has the opposite effect. The inverse time scale is decreased, or as might be expected, a heavier body will take longer to respond.

This timescale can then be used to non-dimensionalize the equation of motion, and to find the relevant dimensionless groups of the problem. If the non-dimensional time, τ, is defined such that $\tau = t(a_1/m^*)(U/D)$, the equation of motion presented in equation 4 can be non-dimensionalized as

$$\ddot{Y} + \frac{m^{*2}}{a_1^2}\frac{kD^2}{mU^2}Y = \left(\frac{1}{2} - \frac{m^*}{a_1}\frac{cD}{mU}\right)\dot{Y} + H.O.T., \tag{12}$$

where $H.O.T.$ represents the higher order terms in $\dot{Y}$. The coefficients can be regrouped into combinations of non-dimensional groups, and rewritten as

$$\ddot{Y} + \frac{4\pi^2 m^{*2}}{U^{*2}a_1^2}Y = \left(\frac{1}{2} - \frac{c^* m^*}{a_1}\right)\dot{Y} + H.O.T, \tag{13}$$

where $c^* = cD/mU$ is a non-dimensional damping parameter.

Equation 13 shows there are four non-dimensional parameters that play a role in setting the response of the system. These are the stiffness (represented by the reduced velocity U^*), the damping c^*, the mass ratio m^*, and the geometry, represented by the rate of change in the aerodynamic force with respect to angle of attack when the body is at the equilibrium position, a_1. The grouping of these parameters into two groups in equation 13 which arise by non-dimensionalising using the natural time scale of the galloping system, suggests there are two groups that dictate the response: $\Gamma_1 = 4\pi^2 m^{*2}/U^{*2}a_1^2$ and $\Gamma_2 = c^* m^*/a_1$. For a given geometry and Reynolds number, Γ_1 can be thought of as a combined mass-stiffness, whereas Γ_2 can be thought of a a combined mass-damping parameter. As it is assumed that during galloping the stiffness plays only a minor role, Γ_2 seems a likely parameter to collapse the data presented in figure 3. In fact, in the classic paper on galloping from **?**, galloping data from wind tunnel tests is presented in terms of a parameter that can be shown to be the same as Γ_2.

All of the quantities that make up Γ_1 and Γ_2 can, in theory, be known before an experiment is conducted. However, the quantity a_1 is a relatively difficult one to determine, requiring static body experiments or simulations. Here, the geometry is unchanged and results are only being compared at the same Re. Hence, suitable parameters can be formed by multiplying Γ_1 and Γ_2 by a_1^2 and a_1 respectively, to arrive at a mass-stiffness parameter $\Pi_1 = 4\pi^2 m^{*2}/U^{*2}$, and a mass-damping parameter defined as $\Pi_2 = c^* m^*$.
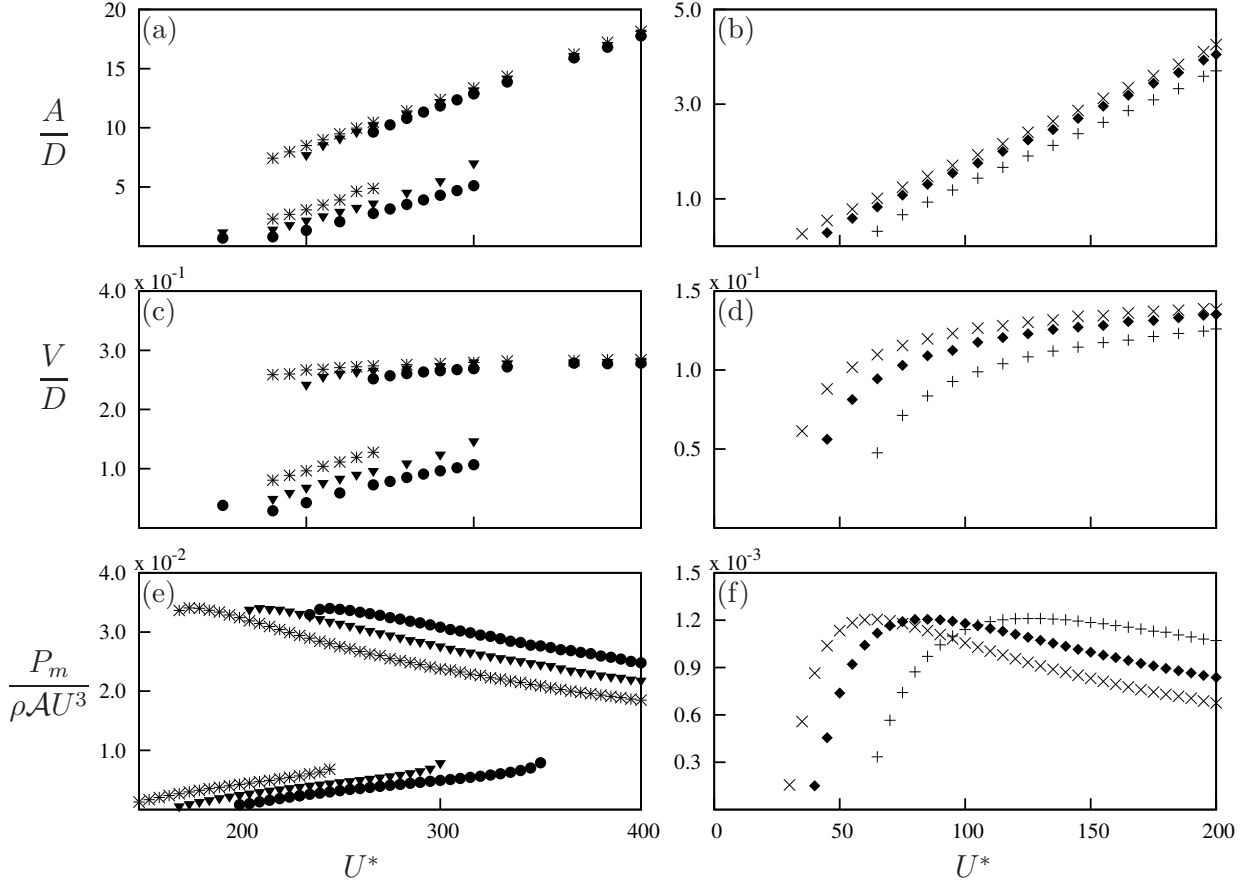
Figure 3: Velocity amplitude, displacement amplitude and mean power as functions of U^*. Data presented in (a), (c) and (e) were calculated using input data at $Re = 22300$ and $m^* = 1163$ obtained by **?** at three different damping ratios: $\zeta = 0.0125$ ($*$), $\zeta = 0.015$ (▼) and $\zeta = 0.0175$ (●). Data presented in (b),(d) and (f) were obtained using input data at $Re = 165$ and $m^* = 20$ at three different damping ratios: $\zeta = 0.075$ (×), $\zeta = 0.1$ (◆) and $\zeta = 0.15$ (+). The multiple branches for the higher Re are due to the hysteresis between two solutions.

The range of incident flow angles where C_y remains positive is narrow at $Re = 200$ ($0° < \theta \leq 7°$) compared to $Re = 22300$ ($0° < \theta \leq 15°$). This feature is what sustains galloping. Power is only transferred from the fluid to the supporting structure within this range of incident angles because fluid forces are acting in the direction of travel of the oscillating body, as demonstrated by equation 6. Incident angles beyond this range actually suppress the galloping and power goes in the opposite direction, i.e; from body to fluid. Therefore due to the overall smaller C_y and narrow range of angles where C_y is positive for $Re = 200$ compared to $Re = 22300$, it is expected that the transferred power at $Re = 200$ is significantly lower than at $Re = 22300$.

3.1. Displacement, velocity and power

A similar result to **?** could be observed in figure 3 (f) where the peak power remains the same but the U^*which corresponds to the peak power shifts to the right as the damping
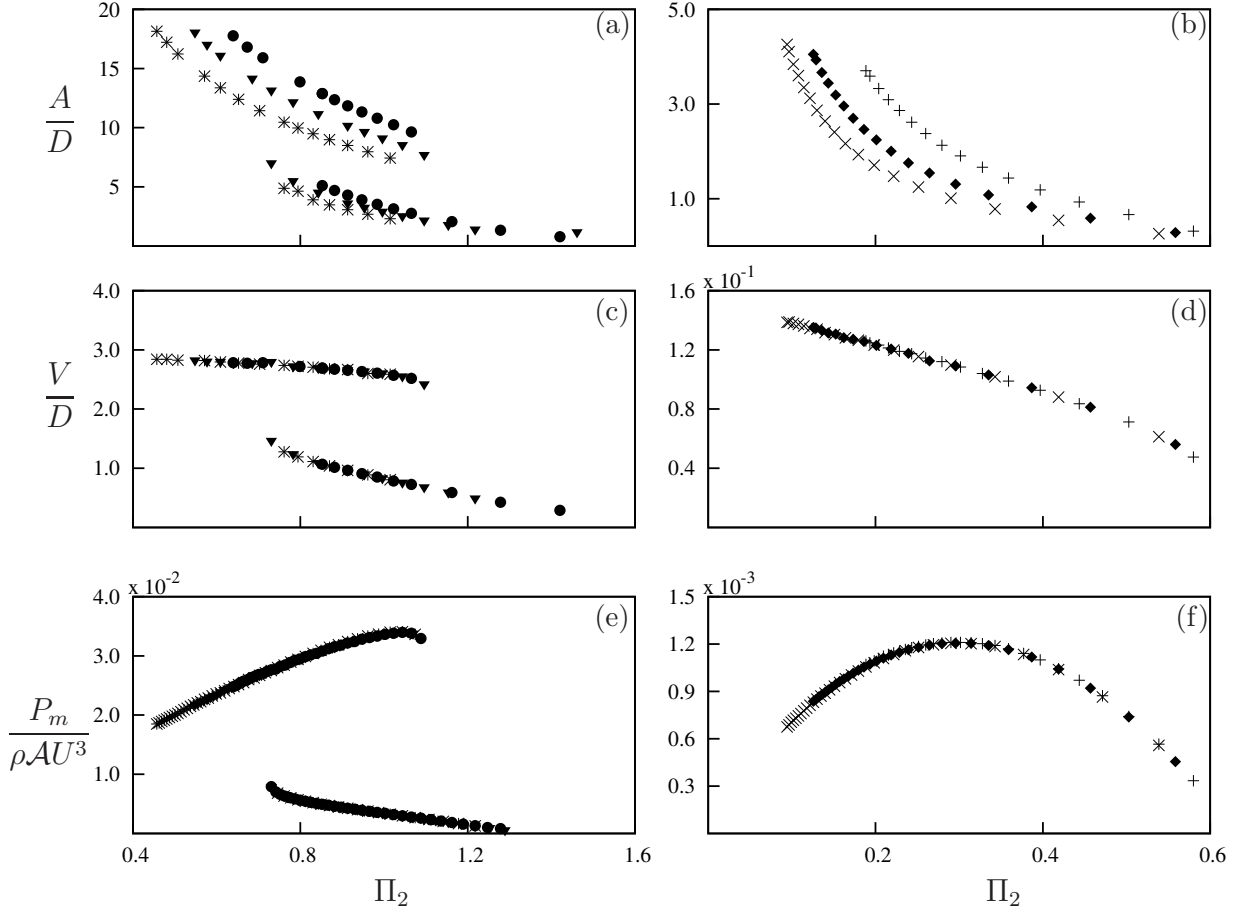
Figure 4: Displacement amplitude, velocity amplitude and mean power as functions of the mass-damping Π_2. Data presented in (a),(c) and (e) were calculated using input data at $Re = 22300$ obtained by **?** at three different damping ratios: $\zeta = 0.0125$ (✳), $\zeta = 0.015$ (▼) and $\zeta = 0.0175$ (●). Data presented in (b), (d) and (f) were obtained using input data at $Re = 165$ at three different damping ratios: $\zeta = 0.075$ (×), $\zeta = 0.1$ (◆) and $\zeta = 0.15$ (+). The collapsed data implies that there is no frequency selection and the tuning parameter of the mechanical side of the system is the damping constant to obtain an optimum power output.
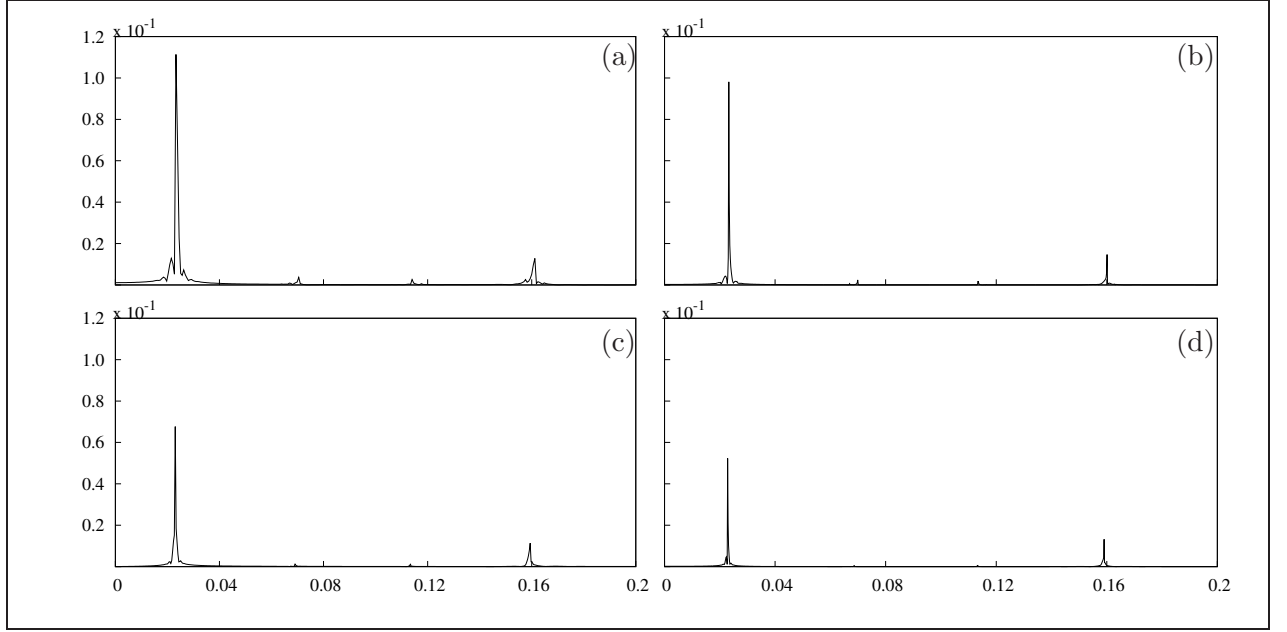
9

Figure 5: Power spectrum of velocity at four different damping levels where (a) $\Pi_2 = 0$, (b) $\Pi_2 = 0$, (c) $\Pi_2 = 0$ and (d) $\Pi_2 = 0$ at $\Pi_1 = 10$ ($U^* = 40$). The two peaks present in the plots represent the galloping signal and the shedding signal where the galloping signal is represented by the large peak. The galloping tends to get weaker as Π_2 is increased while shedding remains constant

ratio is increased. comparing Figures 3 and 4 it is evident that the velocity and mean power data are well collapsed when represented by Π_2 derived using natural time scales earlier in this article compared to the conventional VIV parameters. Thus reinforcing the fact that unlike in VIV power transfer is not bounded by a resonant range of frequencies.

limitation of the quasi-steady hypothesis at low Reynolds numbers Work done by **?** has also been focused on the displacement of a body under galloping at low Reynolds numbers as well as at zero or minimal damping. Therefore studies were carried out analyse the behaviour of the velocity as the damping is increased. The quasi-steady results were compared with the DNS results. From the comparison it was found out that the discrepancy of the power output is quite high as Π_2 is increased.